J. Radiat. Res., 47, 103–112 (2006)

Regular Paper

Development, Beam Characterization and Chromosomal Effectiveness of X-rays of RBC Characteristic X-ray Generator

Satoru ENDO[1], Masaharu HOSHI[1], Jun TAKADA[1], Toshihiro TAKATSUJI[2], Yosuke EJIMA[3], Shin SAIGUSA[4], Akira TACHIBANA[5] and Masao S. SASAKI[5]*

Characteristic X-rays/Ultrasoft X-rays/Chromosome aberrations/RBE.

A characteristic hot-filament type X-ray generator was constructed for irradiation of cultured cells. The source provides copper K, iron K, chromium K, molybdenum L, aluminium K and carbon K shell characteristic X-rays. When cultured mouse m5S cells were irradiated and frequencies of dicentrics were fitted to a linear-quadratic model, $Y = \alpha D + \beta D^2$, the chromosomal effectiveness was not a simple function of photon energy. The α-terms increased with the decrease of the photon energy and then decreased with further decrease of the energy with an inflection point at around 10 keV. The β-terms stayed constant for the photon energy down to 10 keV and then increased with further decrease of energy. Below 10 keV, the relative biological effectiveness (RBE) at low doses was proportional to the photon energy, which contrasted to that for high energy X- or γ-rays where the RBE was inversely related with the photon energy. The reversion of the energy dependency occurred at around 1–2 Gy, where the RBE of soft X-rays was insensitive to X-ray energy. The reversion of energy-RBE relation at a moderate dose may shed light on the controversy on energy dependency of RBE of ultrasoft X-rays in cell survival experiments.

INTRODUCTION

Soft X-rays with energy below 30 keV provide a unique probe for studying the mechanisms of radiation-induced damage to biological systems since their interaction with materials is mostly photoelectric action which produces photoelectrons and Auger electrons with discrete kinetic energy. Soft X-rays are currently available as synchrotron orbit radiations.[1)] However, since the pioneering work of Lea and his colleagues,[2)] low-energy characteristic X-rays have been also successfully used in radiation biology[3)] and have provided significant information on the energy deposition over nano- or micrometer dimensions within living cells and their relevance to cell inactivation, mutation induction, malignant transformation and chromosome aberration formation. Generally, the published data indicate that the relative biological effectiveness (RBE) increases with decreasing of X-ray energy[4–13)] whereas such trend has not been clearly demonstrated in some cell lines.[14–16)] Ultrasoft X-rays strongly attenuate within the cells, resulting in reduction of of dose through a single cell, and hence the average dose absorbed by cell nuclei for a given incident dose is different for thick and thin cells.[3,17,18)] Indeed, equivalent cell inactivation has been reported for iso-attenuating energies of 273 eV and 860 eV X-rays.[19)] However, the experimental methods and interpretation of this latter study have been called into question.[20)] Nevertheless, possible confounding due to cell thickness and dose attenuation does place uncertainties on alternative suggested interpretations that the critical damage is related to the more efficient clustering of energy deposition over nanometer distances with decreasing electron energy[17)] and that biological effectiveness is in a combined function of the linear energy transfer (LET) and the range of electrons.[21,22)]

In the generation of characteristic X-rays, appropriately accelerated electrons or protons striking at the target can eject the orbital electrons of the atoms, and X-rays are emitted when the orbital electrons from higher shells fill the

*Corresponding author: Phone: +81-75-955-8943,
Fax: +81-75-955-8943,
E-mail: msasaki@emp.mbox.media.kyoto-u.ac.jp

[1]Research Institute for Radiation Biology and Medicine, Hiroshima University, Kasumi 1-2-3, Minami-ku, Hiroshima 734-8553, Japan; [2]Graduate School of Environmental Science, Nagasaki University, Bunkyo-machi 1-14, Nagasaki 852-8521, Japan; [3]Hiroshima Prefectural College of Health Science, Gakuen-cho 1-1, Mihara 723-0053, Japan; [4]National Institute of Radiological Sciences, Anagawa 4-9-1, Inage-ku, Chiba 263-8555, Japan; [5]Radiation Biology Center, Kyoto University, Yoshida-konoecho, Sakyo-ku, Kyoto 606-8501, Japan.

inner-shell vacancies giving X-ray energy corresponding to the difference between the electron binding energy of the two shells. The X-ray energies are characteristic of the element of which the target is made and appear superimposed on the continuous energy spectrum of bremsstrahlung. Since the applied voltage is usually several times higher than the desired characteristic X-ray energy, the minimization of the background contamination of bremsstrahlung is particularly important for mechanistic approaches to the biological effectiveness of the characteristic X-rays.

A characteristic X-ray generating system of hot-filament type was constructed in the Radiation Biology Center (RBC) of Kyoto University for the irradiation of cultured mammalian cells as a cooperative research project of the RBC. The system includes the delivery of carbon K (C_K), aluminium K (Al_K), molybdenum L (Mo_L), chromium K (Cr_K), iron K (Fe_K), copper K shell (Cu_K) X-rays. Optimization of beam characteristics and dosimetry were performed, and chromosomal effectiveness was studied in cultured mouse m5S cells. The irradiation system was proven to provide desired characteristic X-rays with a reasonably high dose rate. The chromosomal effectiveness was shown to be dependent on the X-ray energy, which was comparable to those in our earlier[21, 22] and German studies[23] in human peripheral blood lymphocytes irradiated with monochromatized synchrotron radiation.

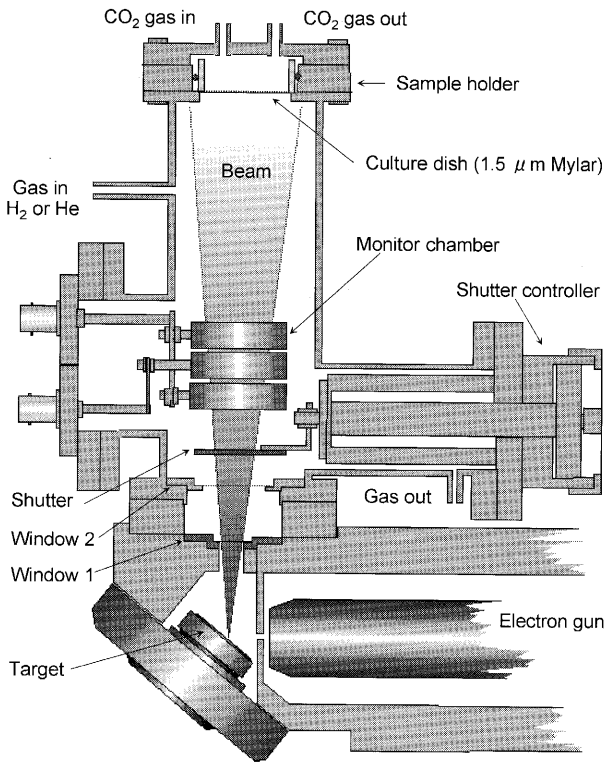

Fig. 1. Cross sectional view of the X-ray tube.

MATERIALS AND METHODS

Characteristic X-ray generator

The outline of the chracteristic X-ray generator is shown in Fig. 1. The X-ray tube is a hot-filament type and consists of replaceable target, replaceable X-ray windows, X-ray shutter, monitor chamber, sample dish holder, and vacuum pumping system with a roughing pump and a turbo-molecular pump to maintain a vacuum below 10^{-4} Pa. The targets included Cu, Fe, Cr, Mo, Al and C. The tube voltage is adjustable from 1 kV to 20 kV in steps of 0.5 kV and the tube current is controlled from 1 mA to 100 mA in steps of 1 mA. The constancy and ripples of the power supply were within 0.1%. The target angle is 40° and the effective beam size is 3.2 mm × 3.2 mm at the focal spot and 4.6 mm × 3.0 mm on the target. The distance from the source to the flight tube window is 240 mm. The X-ray window 1 is either 5 μm, 10 μm or 400 μm thick beryllium depending on the X-ray energy. For the C_K X-rays, 1.5 μm Mylar windows with stainless meshes (200 lines/inch) were used for windows 1 and 2 keeping 10 Pa between them using differential pumping to separate the flight tube from the vacuum X-ray tube. The flight tube is filled with 1 atm of air or a flow of He or H_2 gas at a flow rate of 2 l/min. A cell culture dish with the bottom of 1.5 μm Mylar film is placed in the sample holder. The monitor chamber rings, with a potential difference of 100 V between a central ring and outer rings, are installed in the flight tube to collect ions produced by X-rays transmitted therein. The switching speed of the shutter is less than 0.1 s.

Measurement of energy spectrum

Spectrometry was carried out using a pure germanium X-ray spectrometer (ultralow-energy X-ray detector Model LEGe-GUL0035P, Canberra Industries Inc.). The detector (5 mm thickness, 6.2 mm active diameter, 30 mm^2 active area) has a 0.34 μm thick polymer window, of which 0.04 μm is an aluminium film to block ambient light. The window transmits 10% X-rays at the energy 100 eV. When necessary, absorbers were placed at the sample position in addition to a 1.5 μm Mylar film. Measurements were performed through a 20 μm pin hole in a copper plate or in a lead plate (hole of arbitrary size) placed on window and the output pulses were analyzed with a multi-channel analyzer (Laboratory Equipment Co. 4k MCA installed in NEC Model PC9801RA personal computer). For the energy calibration, the linearity of the MCA channel was confirmed by a pulse generator (ORKEC Model 419) and then 4.952 keV ^{51}V K_α X-rays emitted from ^{51}Cr, and 5.899 keV ^{55}Mn Kα and 6.491 keV K_β X-rays from ^{55}Fe were used as reference X-rays. The X-ray beams were confirmed by characteristic attenuation in air for C_K, Mylar for Al_K and Mo_L, and aluminium for other X-rays.

Measurement of dose rate and field uniformity

The dose rate at the sample position was measured by an extrapolation chamber (Far West Technology Inc., model EIC-1). The extrapolation chamber is a parallel-plate ion chamber with a cylindrical detection volume and a collection area of 0.82114 cm^2. The detection volume is continuously adjustable by moving the spacing plate from 0.3 to 4.5 mm (1 mm/turn). Two thin windows made with graphite-coated 0.7 mg/cm^2 thick polypropylene were used for the dosimetry. The transmission of these two windows was measured for each X-ray beam. The ion chamber currents were measured with the electrometer of a Radocon Dosimeter (Victoreen Model 500). Based on the net-increase of the current, dI, at corresponding plate separation, dR, the absorbed dose was determined using the following equation as described by Hoshi *et al.*.[24]

$$D = 1.602\times10^{-16}\,\mu_t\,\frac{W}{eAT}\,\frac{KdI}{\exp(-\mu_a)[1-\exp(-\mu_a dR)]}\left(1+\frac{dR}{2L}\right)^2, \quad (1)$$

where W is the average energy per ion pair in air, A is the effective collecting area, T is the transmission of the extrapolation chamber window, and e is the electron charge. The parameters, $\mu_a = \rho_a(\mu_{en}/\rho)_a$ and $\mu_t = \rho_t(\mu_{en}/\rho)_t$, are mass attenuation coefficients for air and tissue, respectively. L is the distance from the source to the flight tube window. K is the temperature and pressure correction factor as defined by $K = [1 + C/273](760/P)$ at temperature C in °C and pressure P in mmHg in the ambient condition. The mass attenuation coefficients for the air and ICRU muscle[25] were determined from the tables of mass-energy absorption coefficients of Henke *et al.*[26] for C_K X-rays and of Hubbell[27] for other X-rays. W values were estimated by deduction from the values of electron energy of Combecher[28] assuming pure characteristic X-rays.

The current of the monitor chamber was measured with a current integrator (ORTEC Model 439). The shutter was controlled by a timer-counter (ORTEC Model 771). The field uniformity was determined by exposing photographic films (Konica CS100E) to Al_K X-rays at the flight tube window and scanning the optical density of the developed films using a densitometer (Gelman Model ACD-18) with a slit size 0.1 mm × 2 mm.

Cell culture and chromosome aberration analysis

Cultured mouse m5S cells were maintained in α-modified MEM culture medium supplemented with 10% fetal bovine serum and 20mM HEPES. For irradiation, approximately 5 × 10^5 cells were plated in a Φ30mm culture dish with a 1.5 μm Mylar film base and incubated for 5 or 6 days at 37°C under aeration of 5% CO_2 and 95% air until cells became confluent and arrested at G_1 phase. At this stage, the S phase cells were below 0.1% (Ref. 29). The culture dish was placed in the sample holder and irradiated. After 1 h post-irradiation holding at 37°C for the repair of potentially lethal damage to be completed,[30] the cells were trypsinized and cultured in a Φ100mm dish with fresh medium for 40 hrs including the last 24 hours in the presence of colcemid (0.05 μg/ml). For comparison, m5S cells were similarly grown to confluence in conventional plastic Petri dishes, irradiated with ^{60}Co γ-rays, ^{137}Cs γ-rays and 200 kVp orthovoltage X-rays with a 1 mm Cu filter, and processed for chromosome aberration analysis in the same way. In each series of experiments, the cells were irradiated with 1, 2, 3, 4 and 5 Gy. Chromosome preparations were made according to the C-banding method described previously[29] and dicentric chromosomes were counted in 100–300 cells. The dose-response curves were constructed by the bootstrap method with an iteratively reweighted least squares fitting as described.[31]

RESULTS

Characterization of the irradiation system

The newly constructed characteristic X-ray generator proved to be highly stable and suitable for soft X-ray radiobiology. The properties of the irradiation system were first tested using an aluminium or copper target. The field uniformity at the flight tube window was determined by exposing photographic films with Al_K X-rays at a dose which gave a

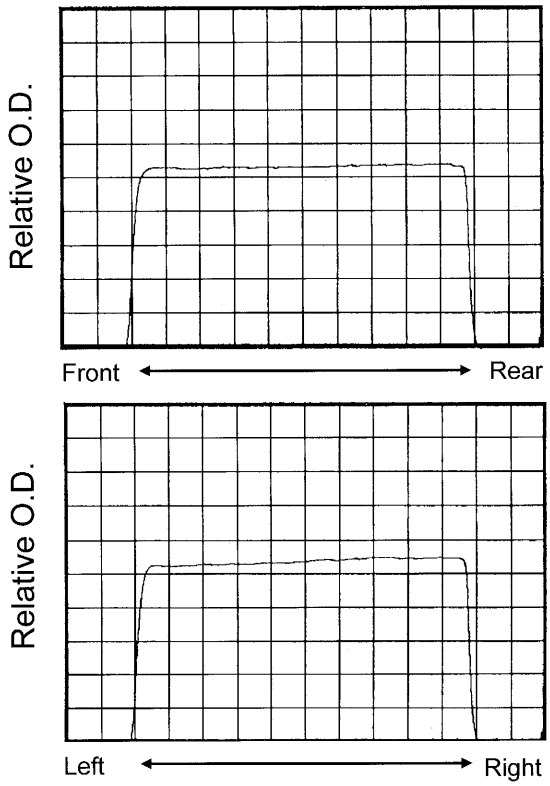

Fig. 2. The dose uniformity at the flight tube window as measured by optical density of photographic films exposed to Al_K X-rays.

half of the maximum optical density. Figure 2 shows the bidirectional distribution of optical density. The dose was uniformly distributed and the dose inhomogeneity at the sample position was less than 3%. In order to minimize the attenuation of X-rays, the flight tube was flushed by He or H_2 gas at a flow rate of 2 l/min. With this flow rate, a full

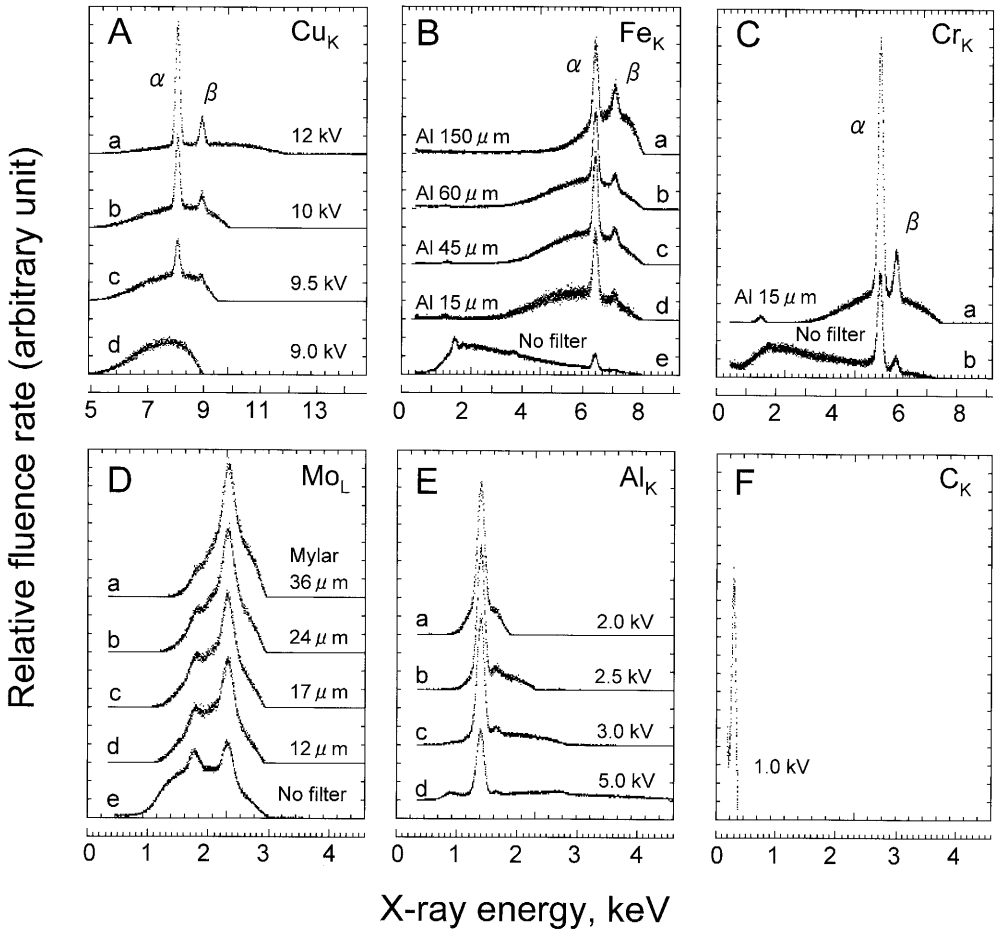

Fig. 3. The energy spectra of the characteristic X-rays and their modulation by changing tube voltage and thickness of added filters. (**A**) Cu_K at indicated tube voltages combined with 150 μm aluminium filter. (**B**) Fe_K at tube voltage of 8 kV combined with indicated thickness of aluminium filters. (**C**) Cr_K at tube voltage of 7.5 kV with or without 15 μm aluminium filter. (**D**) Mo_L at tube voltage of 3.0 kV combined with indicated thickness of Mylar filter. (**E**) Al_K at different tube voltage without additional filter. (**F**) C_K at tube voltage of 1.0 kV without additional filter.

Table 1. Characteristic X-rays and their parameters used in the calculation of the dose.

X-rays	Energy (keV)	$(\mu_{en}/\rho)_{air}$ (cm^2/g)	$(\mu_{en}/\rho)_{tissue}$ (cm^2/g)	*W* value (eV)*)	Transmission (*T*)**)
Cu_K	8.048	9.106	9.622	35.7	0.9958
Fe_K	6.404	19.076	20.046	35.7	0.9958
Cr_K	5.415	30.766	32.389	35.6	0.9958
Mo_L	2.293	394.008	425.472	35.4	0.9636
Al_K	1.487	1230.66	1303.09	35.2	0.8370
C_K	0.277	5180.18	5245.03	33.5	0.7208

*) *W* values were estimated by deduction from the values of electron energy of Combecher[28] assuming pure characteristic X-rays.
**) Transmission of two windows of the extrapolation chamber.

replacement level was achieved within 1 min as determined by the changes in the current reading of extrapolation chamber (data not shown). The monitor chamber was confirmed to be sensitive enough and responded in parallel with the extrapolation chamber, responding to a tube voltage as low as 2 kV for an aluminium target with the discharge current of 5 mA. The current reading was approximately two times higher than that of the extrapolation chamber at the flight tube window.

Optimization of energy spectra and dose rate

To generate the characteristic X-rays, copper (Cu), iron (Fe), chromium (Cr), molybdenum (Mo), aluminium (Al) and carbon (C) were used as targets. The gain of desired characteristic X-rays were tested by changing the tube voltage and selection of added filters. Figure 3 shows the MCA readings of the energy spectra. The best operating condition was obtained by changing the tube voltage alone for Cu_K, Al_K and C_K X-rays. For others, the energy spectra were further modulated by X-ray filters, *i.e.*, aluminum filter for Fe_K and Cr_K and Mylar filter for Mo_L X-rays. The dose rate was determined by changing the collective volume by turning the separation plate of the extrapolation chamber and calculating according to equation (1). The parameters used in the calculation of dose rate are shown in Table 1. The calculated dose rates were consistent for all of 8 different collection volumes (data not shown). They were averaged to determine the dose rate. Table 2 shows the best operating conditions and dose rates for the irradiation of cultured mammalian cells.

Induction of dicentrics in mouse m5S cells

The chromosomal effectiveness of the characteristic X-rays was studied and compared with those for the high-energy γ-rays and conventional orthovoltage X-rays. Small numbers of aberrations were observed in the non-irradiated cultures which were prepared for each experiment and otherwise treated in the same way. The aberrations in the pooled control cultures were 4 dicentrics in 1575 cells (2.54×10^{-3} per cell). Because of low spontaneous frequencies, the

Table 2. The best operating conditions of the characteristic X-rays for cell irradiation.

X-rays	Spectrum*)	Voltage (kV)	Current (mA)	Filtration (added filter)	Dose rate (Gy min^{-1})
Cu_K	A-b	10.0	1	150 μm Al	0.3
Fe_K	B-c	8.0	10	45 μm Al	0.2
Cr_K	C-a	7.5	5	15 μm Al	0.2
Mo_L	D-a	3.0	20	36 μm Mylar	0.65
Al_K	E-b	2.5	10	None	1.8
C_K	F	1.0	5	None	0.1

*) The energy spectra corresponding to those marked in Fig. 3.

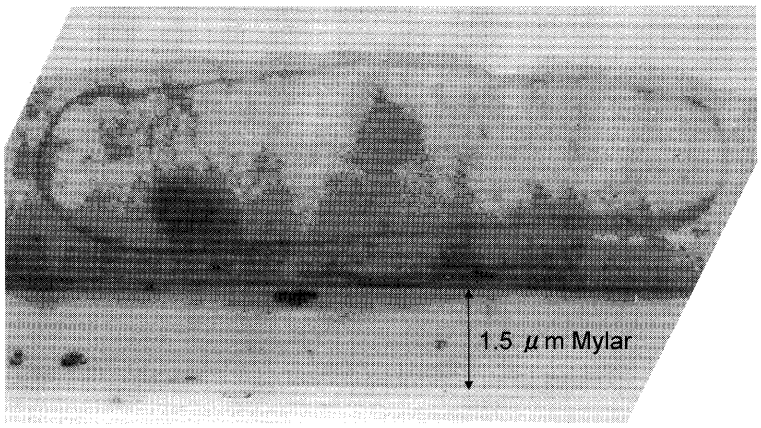

Fig. 4. Cross sectional view of the m5S cell grown to confluence on 1.5 μm thick Mylar substrate. The cells fixed *in situ* on Mylar film sequentially with buffered glutaraldehyde and osmium tetroxide were washed in distilled water, dehydrated in graded series of ethanol and embedded in Epoxyresin as described by Raju *et al.*.[14] Serial sections of 2 μm thick were made and typical slices that were perpendicular to Mylar film and assumed to cross the center of the cells were selected for the measurement of cell thickness on transmission electron micrographs.

frequencies of dicentrics in the irradiated cultures were fitted to a linear-quadratic dose-response model, $Y = \alpha D + \beta D^2$, being constrained to pass through the origin, where Y is aberration frequency on a per cell basis and D is dose in Gy. The dose responses were determined for two-types of doses; one for the surface dose, D_0, incident to the cell surface and another for average nuclear dose, $\overline{D_n}$. The average nuclear dose was estimated by

$$w_n = \frac{\exp\{-(\mu_{en}/\rho)\rho h x_1\}[1-\exp\{-(\mu_{en}/\rho)\rho h x_2\}]}{(\mu_{en}/\rho)\rho h x_2}, \quad \overline{D_n} = D_0 w_n, \tag{2}$$

where x_1 is the thickness of the cytoplasmic layer between the Mylar surface and the nucleus, and x_2 is the thickness of the nucleus. Parameter h is the correction function for the reduction in thickness by fixation. The density of $\rho = 1.04$ for muscle was adopted.[32] The cellular geometry was determined by transmission electron microscopy (Fig. 4). At confluence on a Mylar substrate, the total thickness of the cell was about 3.7 μm, where a 2.8 μm thick nucleus (about 12 μm diameter) was overlaid on a 0.6 μm thick cytoplasmic layer attached to the 1.5 μm Mylar substrate. A maximum reduction in the thickness (20%) in fixed samples of Townsend *et al.*[33] was adopted for the true thickness of the living cells (*i.e.*, $h = 1.2$).

The dose-response relationships of dicentrics are presented in Fig. 5 and Table 3. The dose-response was determined based on the average nuclear dose which was converted from the cell surface dose using the conversion factor, w_n. At the equi-dose level, the aberration frequencies were higher as the photon energy decrease. However, the dose-response kinetics was not simply correlated with the photon energy. As depicted in Fig. 6, α terms increased with the decrease of photon energy down to about 10 keV and then declined with further decrease of the energy. In contrast, the β terms

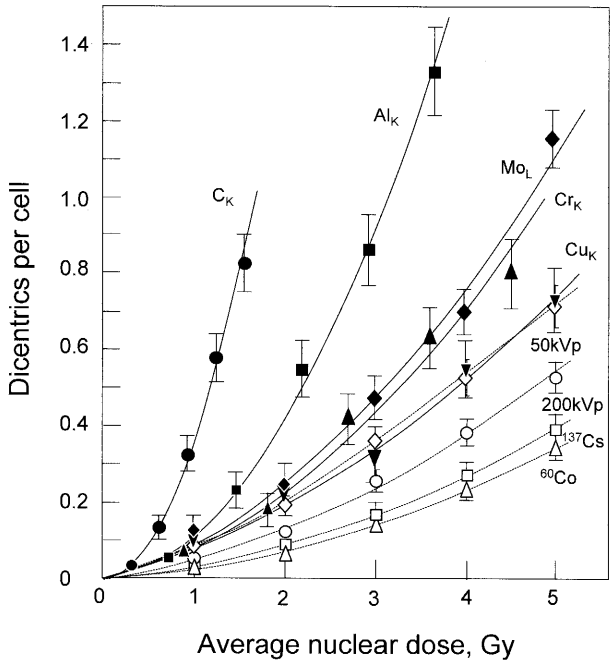

Fig. 5. The dose-response relationships of dicentric chromosome aberrations as a function of average nuclear dose. Vertical lines show the standard errors of the mean. Solid symbols and solid lines show characteristic X-rays. Open symbols and dotted lines show high energy X- and γ-rays. Vertical lines show standard errors of the mean calculated assuming Poisson distribution.

Table 3. Photon energy and dose-response parameters for dicentrics in the mouse m5S cells.

Radiation	Energy	Surface dose			Average nuclear dose			
	(keV)	w_n	α ± S.E. (10^{-2}Gy^{-1})	β ± S.E. (10^{-2}Gy^{-2})	w_n	α ± S.E. (10^{-2}Gy^{-1})	β ± S.E. (10^{-2}Gy^{-2})	RBE_M[**)]
C_K X	0.277	1	0.133 ± 0.260	3.429 ± 0.117	0.310	0.471 ± 1.001	35.790 ± 1.418	0.32 ± 0.69
Al_K X	1.487	1	1.080 ± 0.906	5.185 ± 0.233	0.729	1.438 ± 1.324	9.783 ± 4.641	0.98 ± 0.93
Mo_L X	2.293	1	4.490 ± 1.093	2.588 ± 0.324	0.900	5.126 ± 1.173	3.150 ± 0.389	3.50 ± 1.09
Cr_K X	5.415	1	6.420 ± 2.113	3.084 ± 0.525	0.992	6.448 ± 2.109	3.139 ± 0.525	4.40 ± 1.72
Cu_K X	8.048	1	8.900 ± 1.426	1.114 ± 0.318	0.998	9.087 ± 1.415	1.073 ± 0.318	6.21 ± 1.63
50 kVp X[*)]	11.9	1	5.906 ± 0.635	1.792 ± 0.166	1			4.03 ± 0.96
200 kVp X	97.4	1	3.657 ± 0.415	1.451 ± 0.103	1			2.50 ± 0.60
^{137}Cs γ	662	1	2.239 ± 0.220	1.132 ± 0.053	1			1.63 ± 0.36
^{60}Co γ	1253	1	1.464 ± 0.310	1.080 ± 0.074	1			1

[*)] Previously published data[34] were re-calculated using bootstrap method. The effective energy at 0.2 mm aluminium filter as adopted from Hoshi *et al.*.[35]

[**)] Maximum RBE at low dose limit relative to ^{60}Co γ-rays as reference radiation.

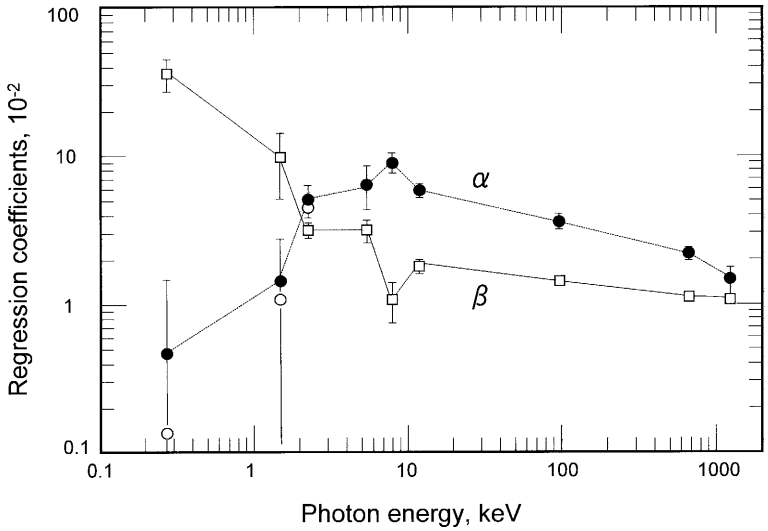

Fig. 6. The changes of α- and β-terms in a linear-quadratic dose-response model against photon energy. Circles: α-terms based on surface dose (open circles) and average nuclear dose (solid circles) ($10^{-2}Gy^{-1}$). Open squares: β-terms based on average nuclear dose ($10^{-2}Gy^{-2}$).

stayed constant down to about 10 keV and then increased with further decrease of the energy. This unique energy dependency has notable similarities to those in human peripheral blood lymphocytes irradiated with monochromatized synchrotron produced radiation.[21–23]

DISCUSSION

A characteristic X-ray generator of hot-filament type was constructed for the irradiation of cultured mammalian cells. The characteristic X-rays include Cu_K, Fe_K, Cr_K, Mo_L, Al_K and C_K X-rays. The best operational conditions were sought by optimizing the tube voltage and adding filtration, and supply of X-rays with reasonably high purity at a high dose rate was confirmed. Throughout its use, the source has been observed to give precisely reproducible exposure. The long-term stability was also confirmed by output measurements before and after a series of experiments; *e.g.*, over a period of at least 6 h of continuous operation.

The source has been successfully used to irradiate cultured mammalian cells. Quantitatively similar results have been obtained for the induction of dicentrics in cultured mouse m5S cells that are comparable to the results in human lymphocytes irradiated with monochromatized synchrotron radiation.[21–23] At least at the equi-dose level, the overall chromosomal effectiveness increased with decreasing photon energy. This is in agreement with observations in many laboratories, mostly using Chinese hamster V79, that ultrasoft X-rays are more effective than high energy X- and γ-rays.[3] Some exceptional cases of insensitivity to X-ray energy[14–16] have been in some way associated with the difference in cell thickness,[18] *i.e.*, thicker cells tend to show higher RBE. The discrepancy could also be somehow related to the localization of dose to a sensitive target site within the cell and/or differing radiosensitivity of cell lines.[17] However, the present observations on the complex dose-response kinetics for the soft X-rays predict a complexity of energy-RBE relations and may shed light on such unsolved conundrums.

By definition, the RBE is expressed by a ratio of the doses of different radiations that give the same effects, *i.e.*, the ratio of doses that satisfies $\alpha_\gamma D_\gamma + \beta_\gamma D_\gamma^2 = \alpha_x D_x + \beta_x D_x^2$ for comparison of X-rays against γ-rays as reference radiation. The RBE of X-rays against γ-rays is thus expressed by

$$RBE = \frac{D_\gamma}{D_X} = \frac{2(\alpha_X + \beta_X D_X)}{\alpha_\gamma + \sqrt{\alpha_\gamma^2 + 4(\alpha_X + \beta_X D_X)\beta_\gamma D_X}}. \quad (3)$$

The RBE is dependent on X-ray dose. Figure 7 shows the changes of RBE with nuclear dose of characteristic X-rays against ^{60}Co γ-rays. For the X-rays with energy higher than 10 keV, the RBE increases with decreasing photon energy because the α-term increases while the β-term is relatively constant ($\beta_x \simeq \beta_\gamma$). However, for the X-rays with lower energies, similar energy dependency can only be seen at the high doses. In the low dose range, the energy dependency is reversed; *i.e.*, the RBE decreases with the decrease of the photon energy. The RBE at low dose and low dose-rate, RBE_M, is thus in the order of $C_K < Al_K < Mo_L < Cr_K < Cu_K$ for energy below 10 keV, and conversely Cu_K > 50 kVp > 200 kVp X-rays > ^{137}Cs γ-rays for energy above 10 keV (Table 3). Such counter energy dependency shifts to a generally observed unidirectional inverse relation to the photon energy as the dose increases. The reversion occurs at doses around 1 to 2 Gy (with the exception of C_K X-rays). Around this crossing dose, the RBE is about 2 to 3 but insensitive to

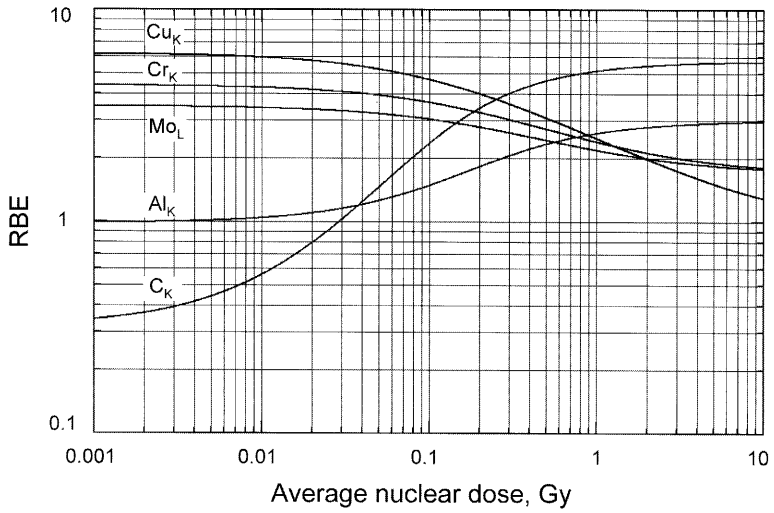

Fig. 7. The calculated RBE of the characteristic X-rays as a function of average nuclear dose. The RBE was calculated according to equation (3) with ^{60}Co γ-rays as reference radiation.

the X-ray energy (excluding C_K X-rays).

In human lymphocytes irradiated with synchrotron-produced monochromatic ultrasoft X-rays,[20,21] the crossing point of dose for RBE is around 0.3 Gy, which is an order of magnitude smaller than that for m5S cells. This difference is due to the different value of β-term while α-terms show notable similarities between the two cell systems. The β-terms in the m5S cells were about 20% of those for human lymphocytes while the overall energy response kinetics were qualitatively similar. The G_0 lymphocyte is a sphere of about 7 μm diameter, about 2 times thicker than m5S cells. There may be less chance for independently formed damage to interact in the thinly spread cell nuclei and hence give rise to a reduced two-track component, *i.e.*, β-term. Since the radiation doses generally used in cell survival experiments are in the order of Gy's, the RBE could be more sensitive to the X-ray energy in thick cells compared with thin cells. The unique energy- and dose-dependency of RBE could be an underlying mechanism of the current discrepancy on the RBE of ultrasoft X-rays. The crossing points of dose for the C_K X-rays appeared at lower doses. The reason for the difference from other X-rays is not clear. However, it could be somehow related to the uncertainty in dose assessment which is intrinsic to the strongly attenuating ultrasoft X-rays.

Photoelectrons generated in the cell nucleus by 0.28 keV C_K X-rays have a CSDA range, a continuously slowing down approximation, of only about 7 nm, which is too short to hit two DNA molecules along a single path of an electron although it might be effective in producing clustered damage leading to double-strand breaks (DSB). This range limitation should be the basis of the reduction of the α-term and concomitant increase in the β-term, *i.e.*, less probability of one-track events and higher probability of two independent track events per unit dose for binary mis-repair of DSBs to lead chromosome exchange aberrations. This contrasts with the high energy X- or γ-rays, where the range of recoil electrons is sufficiently large to hit two DNA molecules as a one-track event, the probability of which is proportional to LET and hence inversely proportional to the energy. The inflection point of X-ray energy may lie at around 10 keV. This is in agreement with the conclusion reported earlier.[21,22] In this interpretation, chromosome exchange aberration formed in G_1 cells is correlated with the pairwise mis-rejoining of two DSBs by non-homologous end-joining (NHEJ). However, it is also necessary to consider an alternative possibility that even a single complex damage event may trigger the exchanges by recruiting undamaged DNA via a homologous recombination (HR) pathway.[36,37] The difference may not lie in the modeling but could be at least in part related to the cell cycle stages at the time of irradiation since NHEJ predominates in the G_1 stage while HR is activated in S and G_2 stages.[38] The cell cycle stage specificity of the two types of repair pathways is in favor of the former mechanism in the cells arrested at G1 stage. The present interpretation also predicts a curvature of the dose response and a strong dose-rate effect for ultrasoft X-rays, which issues remain for further studies.

ACKNOWLEDGMENTS

This work was carried out as a collaborative research project of the Radiation Biology Center, Kyoto University, and was supported by a Grant-in-Aid for the Scientific Research from the Ministry of Education, Science, Culture, Sports and Technology of Japan. We thank RIGAKU Co. Ltd., Tokyo, for cooperation in manufacturing the irradiation system.

REFERENCES

1. Kobayashi, K., Hieda, K., Maezawa, H., Ando, M. and Ito, T. (1987) Monochromatic X-ray irradiation system (0.08–0.4 nm) for radiation biology studies using synchrotron radiation at the Photon Factory. J. Radiat. Res. **28**: 243–253.
2. Lea, D. E. and Catcheside, D. G. (1942) Induction by radiation of chromosome aberrations in Tradescantia. J. Genet. **44**: 216–245.
3. Goodhead, D. T. (1994) Soft x-ray radiobiology and synchrotron radiation. In: Synchrotron Radiation in Biosciences, Eds. B. Chance, J. Deisenhofer, S. Ebashi, D. T. Goodhead, J. R. Helliwell, H. E. Huxley, T. Iizuka, J. Kirz, T. Mitsui, E. Rubenstein, N. Sakabe, G. Schmahl, H. B. Stuhrmann, K. Wutrich, and G. Zaccai, pp.683–705, Oxford University Press, New York.
4. Goodhead, D. T. and Thacker, J. (1977) Inactivation and mutation of cultured mammalian cells by aluminium characteristic ultrasoft X-rays. I. Properties of aluminium X-rays and preliminary experiments with Chinese hamster cells. Int. J. Radiat. Biol. **31**: 541–559.
5. Cox, R., Thacker, J. and Goodhead, D. T. (1977) Inactivation and mutation of cultured mammalian cells by aluminium characteristic ultrasoft X-rays. II. Dose-responses of Chinese hamster and human diploid cells to aluminium X-rays and radiations of different LET. Int. J. Radiat. Biol. **31**: 561–576.
6. Goodhead, D. T. (1977) Inactivation and mutation of cultured mammalian cells by aluminium characteristic ultrasoft X-rays. III. Implication for the theory of dual radiation action. Int. J. Radiat. Biol. **32**: 43–70.
7. Goodhead, D. T., Thacker, J. and Cox, R. (1979) Effectiveness of 0.3 keV carbon ultrasoft X-rays for the inactivation and mutation of cultured mammalian cells. Int. J. Radiat. Biol., **36**: 101–114.
8. Virsik, R. P., Schäfer, Ch., Harder, D., Goodhead, D. T., Cox, R. and Thacker, J. (1980) Chromosome aberrations induced human lymphocytes by ultrasoft Al_K and C_K X-rays. Int. J. Radiat. Biol. **38**: 545–557.
9. Goodhead, D. T., Thacker, J. and Cox, R. (1981) Is selective absorption of ultrasoft X-rays biologically important in mammalian cells? Phys. Med. Biol. **26**: 1115–1127.
10. Folkard, M., Vojnovic, B., Price, K. M. and Michael, B. D. (1987) An arrangement for irradiating cultured mammalian cells with low energy ultrasoft X-rays. Phys. Med. Biol. **32**: 1615–1626.
11. Brenner, D. J., Bird, R. P., Zaider, M., Goldhagen, P., Kliaga, P. J. and Rossi, H. H. (1987) Inactivation of synchronized mammalian cells with low energy X-rays --- results and significance. Radiat. Res., **110**: 413–427.
12. Frankenberg, D., Kühn, H., Frankenberg-Schwager, M., Lenhard, W. and Beckonert, S. (1995) 0.3 keV carbon K ultrasoft X-rays are four times more effective than γ-rays when inducing oncogenic cell transformation at low doses. Int. J. Radiat. Biol. **68**: 593–601.
13. Hill, M. A., Stevens, D. L., Bance, D. A. and Goodhead, D. T. (2002) Biological effectiveness of isolated short electron tracks: V79-4 cell inactivation following low dose-rate irradiation with Al_K ultrasoft X-rays. Int. J. Radiat. Biol. **78**: 967–979.
14. Raju, M. R., Carpenter, S. G., Chmielewski, J. J., Schillaci, M. E., Wilder, M. E., Johnson, N. F., Schor, P. I., Sebring, R. J. and Goodhead, D. T. (1987) Radiobiology of ultrasoft X-rays. I. Cultured hamster cells (V79). Radiat. Res. **110**: 396–412.
15. Schillaci, M. E., Carpenter, S., Raju, M. R., Sebring, R. J., Wilder, M. E. and Goodhead, D. T. (1989) Radiobiology of ultrasoft X rays. II. Cultured C3H mouse cells (10T1/2). Radiat. Res. **118**: 83–92.
16. Cornforth, M. N., Schillaci, M. E., Goodhead, D. T., Carpenter, S. G., Wilder, M. E., Sebring, R. J. and Raju, M. R. (1989) Radiobiology of ultrasoft X rays. III. Normal human fibroblasts and the significance of terminal track structure in cell inactivation. Radiat. Res. **119**: 511–522.
17. Goodhead, D. T. and Nikjoo, H. (1990) Current status of ultrasoft X-rays and track structure analysis as tools for testing and developing biophysical models of radiation action. Radiat. Prot. Dosimet. **31**: 343–350.
18. Carpenter, S., Cornforth, M. N., Harvey, W. F., Raju, M. R., Schillaci, M. E., Wilder, M. E. and Goodhead, D. T. (1989) Radiobiology of ultrasoft X rays. IV. Flat and round-shaped hamster cells (CHO-10B, HS-23). Radiat. Res. **119**: 523–533.
19. Hill, C. K., Nelms, B. E., MacKay, J. F., Pearson, D. W., Kennan, W. S., Mackie, T. R., DeLuca Jr. P. M., Lindstrom, M. J. and Gould, M. N. (1998) Synchrotron-produced ultrasoft X rays: Equivalent cell survival at the isoattenuating energies 273 eV and 860 eV. Radiat. Res. **150**: 513–520.
20. Hill, M. A., Stevens, D. L., Townsend, K. M. S. and Goodhead, D. T. (2001) Comments on the recently reported low biological effectiveness of ultrasoft X rays. Radiat. Res. **155**: 503–510.
21. Sasaki, M. S., Kobayashi, K., Hieda, K., Yamada, T., Ejima, Y., Maezawa, H., Furusawa, Y., Ito, T. and Okada, S. (1989) Induction of chromosome aberrations in human lymphocytes by monochromatic X-rays of quantum energy between 4.8 and 14.6 keV. Int. J. Radiat. Biol. **56**, 975–988.
22. Sasaki, M. S. (1991) Primary damage and fixation of chromosomal DNA as probed by monochromatic soft X-rays and low-energy neutrons. In: The Early Effects of Radiation on DNA, Eds. E. M. Fielden, and P. O'Neill, NATO ASI Series, Vol. H54, pp369–384.
23. Krumrey, M., Ulm, G. and Schmid, E. (2004) Dicentric chromosomes in monolayers of human lymphocytes produced by monochromatized synchrotron radiation with photon energies from 1.83 keV to 17.4 keV. Radiat. Environ. Biophys. **43**: 1–6.
24. Hoshi, M., Goodhead, D. T., Brenner, D. J., Bance, D. A., Chmielewski, J. J., Paciotti, M. A. and Bradbury, J. N. (1985) Dosimetry comparison and characterization of an Al K ultrasoft x-ray beam from an MRC cold-cathode source. Phys. Med. Biol. **30**: 1029–1041.
25. ICRU (1970) Radiation dosimetry: X rays generated at potentials of 5 to 150 kV. International Commission on Radiation Units and Measurements Report 17.
26. Henke, B. L., Lee, P., Tanaka, T. J., Shimabukuro, R. L. and Fujikawa, B. K. (1982) Low-energy X-ray interaction coefficients: Photoabsorption, scattering, and reflection. Atomic

Data Nucl. Data Tables, **27**: 1–144.
27. Hubbell , J. H. (1982) Photon mass attenuation and energy-absorption coefficients from 1 keV to 2 MeV. Int. J. Appl. Radiat. Isot. **33**: 1269–1290.
28. Combecher, D. (1980). Measurement of *W* values of low-energy electrons in several gasses. Radiat. Res. **84**: 189–218.
29. Sasaki, M. S. (2003) Radioadaptive response and genomic instability: a phenotypic dichotomy of genome-environment interaction. In: Radiation and Humankind, Eds. Y. Shibata, S. Yamashita, M. Watanabe, and M. Tomonaga, International Congress Series 1258, pp. 11–19, Elsevier, Amsterdam.
30. Sasaki, M. S., Ejima, Y., Tachibana, A., Yamada, T., Ishizaki, K., Shimizu, T. and Nomura, T. (2002) DNA damage response pathway in radioadaptive response. Mut. Res. **504**: 101–118.
31. Sasaki, M. S. (2003) Chromosomal biodosimetry by unfolding a mixed Poisson distribution: a generalized model. Int. J. Radiat. Biol. **79**: 83–97.
32. Attix, F. H. (1986) Introduction to Radiological Physics and Radiation Dosimetry. John Wiley & Sons, Inc., New York.
33. Townsend, K. M. S., Stretch, A., Stevens, D. L. and Goodhead, D. T. (1990) Thickness measurements on V79-4 cells: a comparison between laser scanning confocal microscopy and electron microscopy. Int. J. Radiat. Biol. **58**: 499–508.
34. Sasaki, M. S. (1995) On the reaction kinetics of the radioadaptive response in cultured mouse cells. Int. J. Radiat. Biol. **63**: 281–291.
35. Hoshi, M., Antoku, S., Russel, W. J., Miller, R. C., Nakamura, N., Mizuno, M. and Nishio, S. (1987) Low energy (soft) X rays: Dosimetry and cell survival. Radiation Effects Research Foundation Technical Report 5–86, 1–26.
36. Griffin, C. S., Hill, M. A., Papworth, D. G., Townsend, K. M. S., Savage, J. R. K. and Goodhead, D. T. (1998) Effectiveness of 0.28 keV carbon K ultrasoft X-rays at producing simple and complex chromosome exchanges in human fibroblasts *in vitro* detected using FISH. Int. J. Radiat. Biol. **73**: 591–598.
37. Dianov, G. L., O'Neill, P. and Goodhead, D. T. (2001) Securing genome stability by orchestrating DNA repair: removal of radiation-induced clustered lesions in DNA. BioEssays, **23**: 745–746.
38. Takata, M., Sasaki, M. S., Sonoda, E., Morrison, C., Hashimoto, M., Utsumi, H., Yamaguchi-Iwai, Y., Shinohara, A. and Takeda, S. (1998) Homologous recombination and non-homologous end-joining pathways of DNA double-strand break repair have overlapping roles in the maintenance of chromosomal integrity in vertebrate cells. EMBO J. **17**: 5497–5508.

Received on November 18, 2005
Revision received on February 14, 2006
Accepted on February 27, 2006